Performance Evaluation of Scanning Electron Microscopes using Signal–to–Noise Ratio

Naresh Marturi[#] , Sounkalo Dembélé, and Nadine Piat

FEMTO–ST Institute, AS2M Department, UMR CNRS 6174 – UFC / ENSMM / UTBM, Besançon, France
Corresponding Author E–mail: naresh.marturi@femto–st.fr, TEL: +33–381 402 913, FAX: +33–381 402 809

KEYWORDS: Scanning Electron Microscopes, Image Signal-to-Noise ratio

Scanning Electron Microscope is becoming a vital imaging tool in desktop laboratories because of its high imaging capability. Through this work we evaluate the performance of two different SEMs consisting of a tungsten gun and a field effect gun, with respect to time and magnification by estimating their image signal-to-noise ratio. SNR is mainly applied to quantify the level of image noise over changes in the acquisition time and magnification rates. Majority of the existing methods to estimate this quantity are based on cross-correlation technique and requires two images of the same specimen area. In this paper we propose a simple and efficient technique to compute signal-to-noise ratio using median filters. Unlike other techniques the proposed method uses only a single image and can be used in real time applications. The derived results show the effectiveness of the developed algorithm.

NOMENCLATURE

FIB = Focused Ion Beam
SEM = Scanning Electron Microscope
TEM = Transmission Electron Microscope
GIS = Gas Injection System
SNR = Signal-to-Noise Ratio
FEG = Field Effect Gun
SE = Secondary Electron
BSE = Back Scattered Electron
ACF = Auto Correlation Function
I,S,N = Acquired, signal and noise images
STD = Standard deviation

1 Introduction

The control of machining provided by FIB facilitates a fast expansion of desktop laboratories dedicated to the preparation of S/TEM samples. These laboratories commonly include a FIB, a GIS, a robot manipulation system and a SEM. The FIB performs machining to obtain a very thin specimen transparent to electrons and the width varying between $500nm$ and $10nm$. It also enables cutting of samples before transferring them to the final support. The GIS performs the deposition or removal of matter by SEM electron beam or by FIB. The robotic system performs the lift-out i.e. picking up a sample from the primary matrix, transferring and placing on the final support. All these elements are positioned inside the SEM chamber that supplies adequate level of vacuum and cleanliness for the overall processing [1]. Besides sample preparation, a SEM based desktop laboratory can be used to perform dynamic analysis and characterization of samples to retrieve their structural, mechanical, electrical or optical properties. Both applications sample preparation and analysis require long operation times and also a change in SEM magnification to fit the accuracy of measurements as well as the field-of-view.

Moreover, SEM is a powerful imaging instrument used in a variety of applications mainly because of its capability in providing images with high resolution and magnification ranges. These images are produced by detecting and converting various signals emitted during the electron beam - specimen interaction [2]. They are used to provide a dynamic visual feedback and real-time monitoring of the working scene in order to perform the assembly/handling task [3].

However, to perform an autonomous micro-manipulation of a sample ($< 10\mu m$) using a SEM based desktop factory, the primary requirement is that the quality of acquired images is high enough (i.e. having less percentage of noise) to be exploitative. One main indicator of the acquired image quality is the SNR mainly because of its efficiency in quantifying the level of noise in an image.

SNR is a commonly used measure in the field of signal processing to estimate the strength of a signal with respect to the background noise. So far, two microscope images of the same specimen area have been used in many research works to compute the SNR based on cross-correlation technique [4, 5]. The primary disadvantage associated with the used methods is that they require two images to be perfectly aligned and in ad-

dition, requires long processing times which makes them difficult to use in real-time applications. Apart from that for SEM imaging, if a sample is scanned for too long by probe it may become contaminated and unusable. Thong [6] used a single image to compute the SNR based on the simple approximation and first-order extrapolation. Even though the results are good enough but the used method is highly dependent on the nature of images.

In this work, assuming the level of noise is high and presence of the image drift, we overcome the above difficulties by developing a simple and robust noise estimation method based on non-linear filtering and then computing the SNR using a single image. In turn, it is used to estimate the SEM's performance in real-time at varying time and magnification rates. This work is mainly aimed to evaluate various SEMs and to choose an available best configuration for the future vision based autonomous micro sample handling process. It is also used to quantify any SEM with respect to the noise.

This paper is organised as follows. The basic concepts of SEM imaging are described in Section 2. In Section 3 we present the related work regarding SNR computation along with the proposed method. Experiments with the system and results are shown in section 4 followed by the conclusion.

2 SEM Imaging

The two different SEMs used for this work are JEOL JSM 820 with a tungsten filament gun and Carl Zeiss Supra with a FEG. The important difference between them is the maximum possible resolution with a tungsten gun SEM is $10nm$ whereas for a FEG it is $1nm$. Conventionally, a SEM consists of an electron column equipped with an electron gun (to produce a continuous beam of electrons), a sample chamber with a positioning stage and different electron detectors for detecting various types of emitted electrons during probe-sample interaction. The apertures and coils present inside the column are responsible to reduce the generated beam diameter, accelerate and focus the beam on the supplied scanning surface of a specimen. The basic construction of the column is shown in the Figure 2.1.
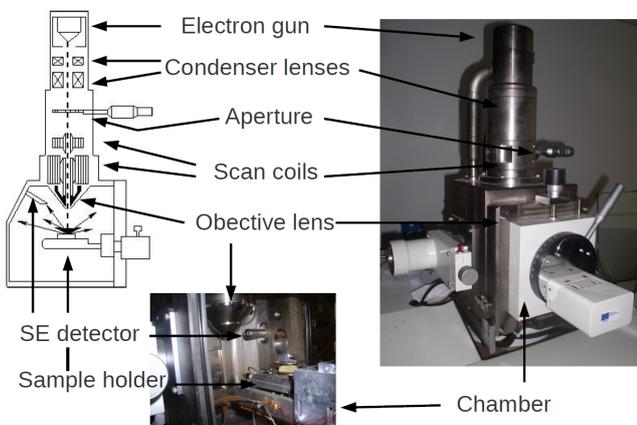
Figure 2.1: SEM electron column construction in reference with JEOL SEM

SEM images are formed by raster scanning the specimen area with produced electron beam and by recording the emitted electron information during this process. Later the gathered information is amplified and displayed on the monitor. SEM produces two dimensional gray scale images. The

main advantage with a SEM is its ability in producing images with high depth-of-field and magnification. Typically, the magnification rates vary from $25\times$ to $250,000\times$. The image resolution can be changed by changing the probe current and the acquisition time. In general, the common trade-off for image resolution in electron microscopy is the image SNR. The quality of the images produced can be expressed in terms of SNR. Operationally, high quality images can be acquired by increasing the beam current or by increasing the scanning time.

The images produced by a SEM are classified into different types based on the emitted electrons. Commonly used image types for most of the micro/nano applications are SE and BSE images. In this work, SE images have been used. Figure 2.2 shows a sample SE image of a standard gold on carbon sample. Normally the SE images are result of inelastic collisions and scattering of incident electrons with the electrons present on specimen surface. These images mainly provide the surface topographical information. More information about the other image types can be found in [2].
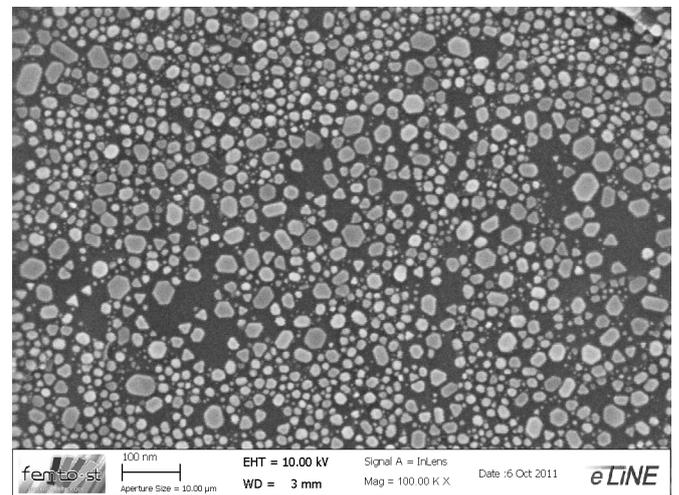
Figure 2.2: SE image of gold on carbon sample at 100k× magnification

However, SEM image acquisition is known to be affected by the addition of noise during beam production, its interaction with the sample and also by the presence of instabilities and non-linearities in the electron column during the scanning process [7]. At low scanning times the level of noise in the images is high in turn reducing the level of SNR. Moreover, noise can also be added by the charge-up of specimen surfaces due to continuous scanning by electron beam and also by mechanical vibrations. This work mainly focus on selecting the best possible quality images over time and magnifications based on the image SNR to estimate the variance of noise under the particular instrument in use.

3 SNR computation

SNR is one of the commonly used quantitative measures in the context of image quality as a measure of image noise. Many applications like image restoration, noise filtering algorithms use this parameter for estimating the noise variance [8]. Mainly with SEM SE imaging, the quantification of SNR is an important task where the images are possibly degraded by noise. SNR provides the level of original details present in the image in comparison with the level of noise. The higher the value of SNR the better the quality of acquired image. Following the

industry standards, SNR can be defined as

$$SNR \triangleq 10\log_{10} \frac{variance\{signal\}}{variance\{noise\}} \qquad (3.1)$$

3.1 Related work

One of the most commonly used methods to compute SNR is by using image cross correlation technique [4]. However in order to use this method, two perfectly aligned microscopic images of the same specimen area are required. This approach assumes that the drift effects are negligible and only noise varies between images. Thong [6] proposed a single image SNR estimation method using the same technique by assuming that the noise in the image is additive white noise. Later, the ACF is computed for the corrupted image from which the noise and noise free peaks are estimated using interpolation. Figures 3.1a and 3.1b shows the ACF and 2 dimensional ACF curve taken along x-axis respectively for the sample image shown in Figure 2.2.
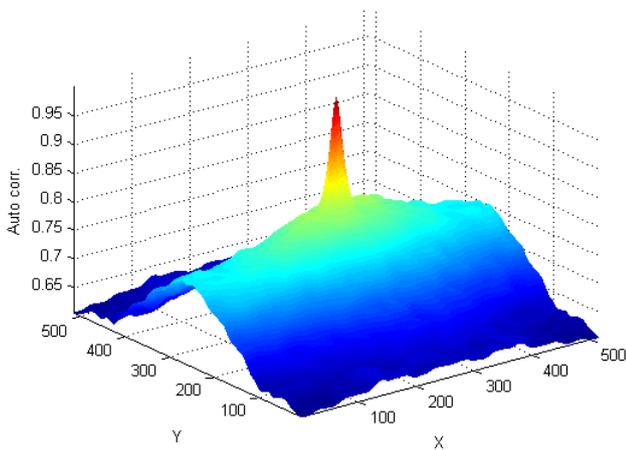
Figure 3.1a: ACF curve for the image shown in Figure 2.2
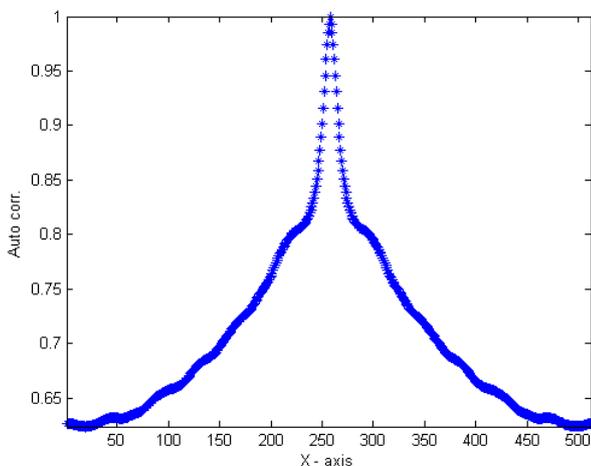
Figure 3.1b: ACF curve along x-axis

From the computed ACF, noise free peak is found using interpolation. Figure 3.2 shows the two peaks. The SNR is described as:

$$SNR = \frac{Noise\,free\,peak - (mean(pixels))^2}{Noise\,peak - Noise\,free\,peak} \qquad (3.2)$$

It is difficult to use the above method for online applications mainly because of the reason that the Overal computational time is more. Moreover, accuracy of the method is highly dependent on noise free peak estimation.
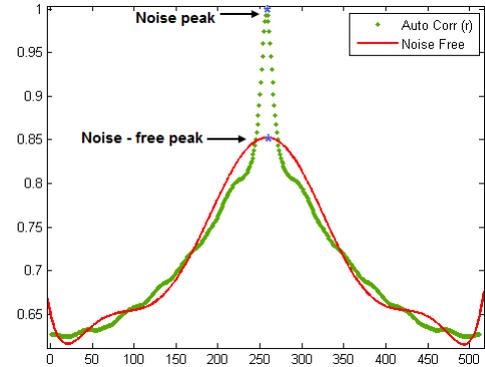
Figure 3.2: Estimated noise and noise free peaks

To overcome the drawback associated with the above method, a simple technique using single image to estimate the SNR for online applications is implemented based on noise filtering by convoluting the image with a nonlinear filter kernel. By comparing all the available nonlinear filter masks like Gaussian, median etc., median filtering seem to provide best performance in filtering the noise and preserving image details [9]. Even though Gaussian is good at filtering noise, it removed fine image details like sharp edges. The proposed method is explained below.

3.2 Proposed approach

Assuming the acquired image is corrupted by spatially uncorrelated additive Gaussian white noise [5, 6, 10] the image model is given by

$$I(x,y) = S(x,y) + N(x,y) \qquad (3.3)$$

Each captured frame undergoes histogram equalisation as a step of normalising the intensity levels and enhancing the image contrast. This is an optional step as the software provided with modern SEMs includes this functionality directly while acquiring the images. The normalised image is then convoluted with a median filter of appropriate size in order to reduce the noise effects. In detail, each pixel in the image is replaced by the median value of its surrounding neighbourhood. The size of the filter is chosen by trial and error. Figures 3.3a and 3.3b shows the resulting filtered image, S and removed noise image, N respectively for Figure 2.2.
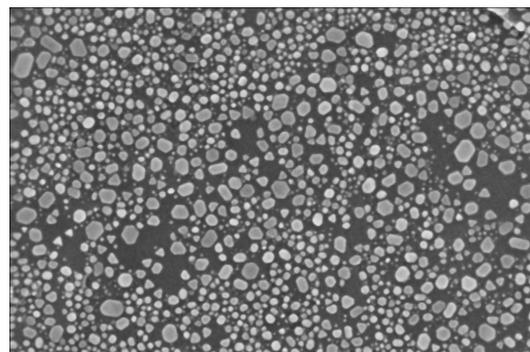
Figure 3.3a: Filtered image

Figure 3.3b: Noise image

Figure 3.4b: Image corrupted with Gaussian noise of 20dB

Using S, the noise can be formulated by subtracting S from I resulting in N. In turn both S and N are used in computing SNR. The final SNR following industry standards of $20 \log_{10}$ can be defined as:

$$SNR = 20 \log_{10} \frac{STD(S)}{STD(N)} \qquad (3.4)$$

A specimen is positioned upon the positioning stage inside SEM vacuum chamber. A set of images are acquired from t_0 to t_f with a sampling time T for each magnification ranging from g_0 to g_f with a sampling step of G. The SNR quantification using the proposed approach is described in algorithm 3.2.

Algorithm 3.2 Algorithm for SNR quantification

1: **for** $g = g_0 \rightarrow g_f$ **do**
2:     **for** $t = t_0 \rightarrow t_f$ **do**
3:         Acquire image, I;
4:         Normalise intensity levels;
5:         Apply median filter to get S;
6:         I-S to get N;
7:         Compute SNR using 3.4;
8:     **end for**
9: **end for**

The robustness of the proposed method is evaluated by corrupting a noise free image shown in Figure 3.4a with additive white Gaussian noise for which the SNR level is known prior to the addition. Later the SNR is computed from the corrupted image using proposed method and is compared with the original values in order to test its efficiency. Table 3.1 shows the original and obtained SNR values.

Figure 3.4a: Noise free image

Table 3.1: **Original and obtained SNR values**

Original SNR (dB)	Obtained SNR (dB)
15	14.3743
16	15.2436
17	17.2480
18	18.1332
19	19.5319
20	20.0264
21	21.0056
22	21.8679
23	22.6670
24	23.7125
25	24.6833
26	25.2426
27	26.7032
28	27.9277
29	28.6508
30	29.4661

From the obtained results it is clear that the proposed method has a reliable performance in estimating the noise level from a given corrupted signal as well as in computing SNR values.

4 Evaluation and discussion

The performance of two different SEMs Jeol JSM 820 and Carl Zeiss Supra is evaluated using the proposed approach. It uses SE images of standard Gold on Carbon sample with low voltage resolution ($30nm - 500nm$) for Jeol SEM as it is an aged SEM and normal resolution ($5nm - 150nm$) for Carl Zeiss SEM.

The accelerating voltage used to accelerate the produced beam is 10kV and the magnifications used for this work are ranged from $10k\times$ to $100k\times$ with an increase of 10k. For each magnification $20 - 30$ images are acquired with a sampling time of 30 seconds i.e. a single image is captured for every 30 seconds. Chosen image size for this work is 512×512. Once an image is acquired its SNR value is computed using algorithm 3.2.

The evaluation process is performed in two steps. The primary step is to estimate the SEM performance with increase in time. Tables 4.1 and 4.2 summarises the obtained SNR values (in dB) for different magnifications with increase in time (30 seconds for each count) for tungsten gun SEM (Jeol) and FEG SEM (Carl Zeiss Supra). Sample plots comparing the SNR levels with both the SEMs at different magnifications are shown in the Figures 4.1 and 4.2.

Table 4.1: SNR values (in dB) for Jeol SEM

Magnification rates				
10000×	15000×	20000×	25000×	30000×
17.4536	18.9045	17.7562	20.8551	19.5582
17.4708	18.9635	17.8127	20.8353	19.6026
17.5719	18.9120	17.8672	20.7796	19.6623
17.5645	18.9678	18.9029	20.8866	19.6288
17.7280	18.9216	18.9257	20.9368	19.7071
17.7317	18.9774	18.9626	20.0229	19.7394
17.7580	18.9923	18.9819	20.1088	19.7572
17.7815	19.0035	18.0084	20.1029	19.8194
17.8303	19.0058	18.0263	20.2038	19.8408
17.8454	19.0827	18.0523	20.2695	19.8644
17.8698	19.0426	18.0831	20.2787	19.8408
17.9208	19.1212	18.1636	20.3237	19.8904
18.0420	19.1128	18.2382	20.3480	19.8707
17.9926	19.1868	18.2554	20.3478	19.9000
18.0404	19.1412	19.2752	20.3786	20.9191
18.0637	19.1544	19.2871	20.3900	20.9219
18.1012	19.1549	19.2466	20.3842	20.9297
18.1205	19.1755	19.3011	20.3497	20.9101
18.1626	19.1797	19.3197	20.3293	20.9209
18.1596	19.1864	19.3117	20.3190	20.8867

Table 4.2: SNR values (in dB) for Carl Zeiss SEM

Magnification rates				
60000×	70000×	80000×	90000×	100000×
17.3942	16.9059	15.4394	16.2897	16.6367
17.8734	16.9669	15.5451	16.4657	16.9874
18.2265	17.1716	15.5451	16.4657	17.2667
18.6786	17.1716	15.8911	16.8509	17.4951
18.7267	17.6672	15.9604	16.9306	17.6999
18.9605	17.8276	16.0912	17.1262	17.8748
19.1688	17.9797	16.2547	17.3217	18.0521
19.2134	18.0416	16.3372	17.4020	18.2933
19.3825	18.1382	16.4224	17.4020	18.4179
19.2693	18.2387	16.4833	17.8535	18.5065
19.5012	18.3103	16.6785	17.9680	18.4610
19.8314	18.4442	16.7113	18.1125	18.5710
20.0031	18.4381	16.9536	18.2303	18.7546
19.8055	18.7222	16.9712	18.3546	18.7331
20.6075	18.6924	17.0032	18.4183	18.8932
20.8755	18.7884	17.0457	18.6238	18.9844
20.8318	18.8678	17.1389	18.6963	19.0937
20.8405	18.9278	17.1812	18.8157	19.0546
21.0915	19.0026	17.4818	18.9375	19.2215
20.9610	19.4176	17.4339	19.0563	19.3941

Figure 4.2: Acquisition time vs. SNR at 70,000 × magnifications

After evaluating the two SEMs, it is observed that the level of SNR is increased with increase in time. And also it is clear from the Figures 4.1 and 4.2 that the SNR level is weak for Jeol SEM in comparison with Zeiss SEM. However, in every case the SNR level is high enough (>15dB) to make the images exploitable. Next, the SEMs performance is evaluated with increase in magnifications and the results are summarised in Figures 4.3 and 4.4 for Jeol and Carl Zeiss SEMs respectively.
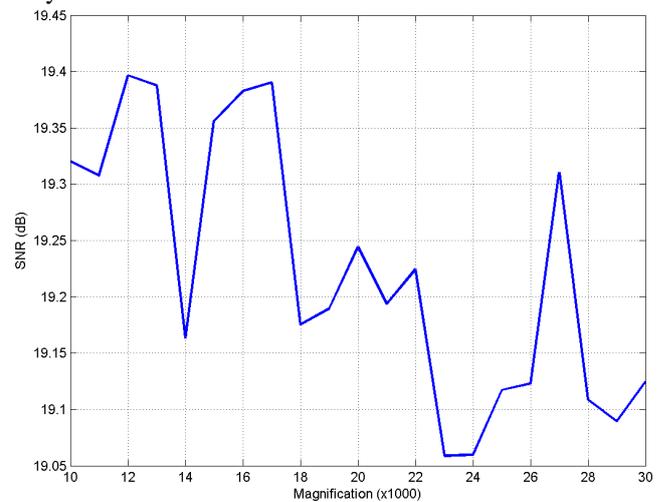
Figure 4.3: Magnification vs. SNR for Jeol SEM

Figure 4.1: Acquisition time vs. SNR at 40,000 × magnifications
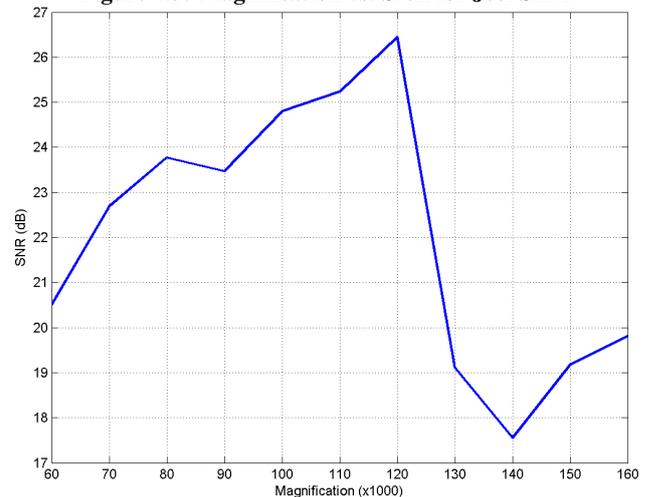
Figure 4.4: Magnification vs. SNR for Carl Zeiss SEM

The results obtained shows that, unlike with time the level of SNR decreases with increase in magnification rates. From figure 4.3 we can say that this rate of decrease is comparatively negligible for Jeol SEM.

5 Conclusion

In this paper, we evaluate the performance of two different SEMs with respect to time and magnification using image SNR. After evaluation it is clear that the FEG SEM (Carl Zeiss) shows better performance or imaging abilities in comparison with the SEM containing a tungsten gun (Jeol). The results obtained show that the level of SNR increases with respect to time for both the SEMs, but the rate of increase is more for the FEG SEM than the tungsten gun SEM.

To compute image SNR a new, simple and fast method based on median filtering has been proposed. It overcomes the difficulties associated with various other SNR computation algorithms by using only a single image. As the time taken for overall process is very less the proposed method can be used with real time applications. The obtained results show the effectiveness of the proposed algorithm.

REFERENCES

[1] J. Dai, S. Tee, C. Tay, Z. Song, S. Ansari, E. Er, and S. Redkar, "Development of a rapid and automated tem sample preparation method in semiconductor failure analysis and the study of the relevant tem artifact," *Microelectronics journal*, vol. 32, no. 3, pp. 221–226, 2001.

[2] J. Goldstein, D. Newbury, D. Joy, C. Lyman, P. Echlin, E. Lifshin, L. Sawyer, and J. Michael, *Scanning electron microscopy and X-ray microanalysis*, vol. 1. Springer Us, 2003.

[3] T. Sievers and S. Fatikow, "Visual servoing of a mobile microrobot inside a scanning electron microscope," in *Intelligent Robots and Systems, 2005.(IROS 2005). 2005 IEEE/RSJ International Conference on*, pp. 1350–1354, IEEE, 2005.

[4] J. Frank and L. Al-Ali, "Signal-to-noise ratio of electron micrographs obtained by cross correlation," *Nature*, vol. 256, pp. 376–379, 1975.

[5] K. S. Sim, M. E. Nia, and C. P. Tso, "Image noise cross-correlation for signal-to-noise ratio estimation in scanning electron microscope images," *Scanning*, vol. 33, no. 2, pp. 82–93, 2011.

[6] J. Thong, K. Sim, and J. Phang, "Single-image signal-to-noise ratio estimation," *Scanning*, vol. 23, no. 5, pp. 328–336, 2001.

[7] M. Abed, D. Sounkalo, P. Nadine, A. Claire, and M. Naresh, "Toward fast calibration of the global drift in scanning electron microscopes with respect to time and magnification," *International Journal of Optomechatronics*, vol. 6, no. 1, pp. 1–16, 2012.

[8] T. Bose, F. Meyer, and M. Chen, *Digital signal and image processing*. J. Wiley, 2004.

[9] R. Gonzalez and R.E.Woods, *Digital Image Processing*. Pearson Prentice Hall Press, New Jersey, 3 ed., 2008.

[10] N. Kamel and S. Kafa, "Image snr estimation using the autoregressive modeling," in *International Conference on Intelligent and Advanced Systems (ICIAS), 2010*, pp. 1–5, IEEE, june 2010.